

# Discontinuous and continuous coarsening of lamellar precipitates in Cu–Be alloys

H. TSUBAKINO, R. NOZATO, A. YAMAMOTO

*Himeji Institute of Technology, 2167 Shosha, Himeji, Hyogo 671-22, Japan*

A study has been conducted of the coarsening reaction which occurs after discontinuous precipitation in Cu–Be alloys. When the discontinuous precipitation is nearly complete, a secondary cellular reaction with much coarser interlamellar spacing forms at the original grain boundaries and advances into the primary cells. The growth rate decreases and the interlamellar spacing increases with the cell growth for the secondary reaction. These phenomena are attributed to the continuous coarsening reaction which simultaneously occurs in the primary cells. The  $\alpha$  phase in the cells produced by the first reaction is supersaturated at the initial cell growth, but attains its equilibrium concentration prior to the appearance of the secondary cells. Cold work does not influence the cell growth of the secondary reaction. The driving force for the secondary reaction is the reduction in total interlamellar surface energy.

## 1. Introduction

A discontinuous coarsening, secondary cellular reaction, associated with lamellar products has been observed in many alloy systems, including eutectic solidification [1–4], eutectoid transformations [5–8] and discontinuous precipitation [9–18].

Theoretical models of cell growth in the discontinuous coarsening reaction have been developed by Livingston and Cahn [6] and Fournelle [11, 12]. The Livingston and Cahn model is based on the assumption that the driving force for the secondary cell growth is the surface energy term, i.e. the reduction in total interlamellar surface energy. The latter theory also takes into account the driving force for the secondary cell growth obtained from the chemical energy term which comes from the degree of supersaturation of solute remaining in the depleted matrix in the primary lamellar structure.

Studies of experimental growth kinetics have shown that the surface energy term will be dominant in all eutectic and eutectoid alloys. In a study of discontinuous precipitation, the chemical energy and surface energy terms have been considered in Ni–Sn [9], Fe–Zn [10], Fe–Ni–Ti [11–13] and Al–Zn [14] alloys and the surface energy term in Pb–Na [15] and Cu–Be [16] alloys. Usually, the solute content in the depleted matrix within the primary cells during initial cell growth is higher than that of the equilibrium state. But the secondary cells advance into the primary cells at a much later ageing stage, when a continuous coarsening reaction will occur [18, 19].

However, there are few systematic studies on cell growth parameters, i.e. the interlamellar spacing and solute content of the depleted matrix of primary cells, during the later ageing stages. In particular, measurements of these parameters have not been studied in regions adjacent to the advancing interfaces of second-

ary cells, therefore preventing experimental identification of the driving force for the secondary reaction.

The discontinuous coarsening reaction of lamellar precipitates ( $\alpha + \gamma$ ) in Cu–Be alloys has been studied [16–18]. The present paper presents further results on the variations of cell growth parameters with ageing time in both the secondary cells and primary cells adjacent to the advancing interface, in order to investigate the driving force problem for the discontinuous coarsening reaction.

## 2. Experimental procedure

The two Cu–Be alloys containing 9.8 and 13.4 at % Be which were investigated were the same alloys as employed in the previous studies on the discontinuous precipitation [21–23]. The alloys were hot forged and then hot- and cold-rolled to plates of  $\sim 3$  mm thickness. The plates were annealed for 72 ks at 1073 K in an argon atmosphere to obtain a uniform grain size. Specimens ( $\sim 10 \times 10 \times 3$  mm<sup>3</sup>) were then solution annealed for 3.6 ks at 1073 K in an argon atmosphere, quenched into iced water, and then aged isothermally. Ageing treatments were carried out in molten salt baths maintained to within  $\pm 2$  K. The ageing temperatures ( $T_A$ ) studied were 673, 723 and 773 K. To study the influence of cold work on the cell growth behaviour of the secondary reaction, the aged specimens were quenched into iced water and cold-rolled up to 20% reduction in area (RA) at room temperature and then reaged.

The variations in cell radius,  $R$ , interlamellar spacing,  $l$ , and the volume fraction of  $\gamma$  phase within cells,  $f_\gamma$ , with ageing time were determined by the methods reported previously [21–23], i.e.  $R$  is taken as the largest distance perpendicular to original grain boundary from advancing cell boundary,  $l$  is taken as

the minimum spacing and  $f_\gamma$  is determined by the point counting method.  $l$  and  $f_\gamma$  in the primary cells were carefully measured from the regions close to the advancing interface of secondary cells when the secondary cells were observed, and from the regions near original grain boundaries when no secondary cells were observed.

Hardness was measured using a micro-Vickers hardness tester applying a 0.98 N load in both regions of primary and secondary cells.

### 3. Results

#### 3.1. Microstructure

Typical microstructures of cellular structure during the first and second stages are shown in Fig. 1. The cells produced by the initial reaction form at the grain boundaries and advance into the grain interiors, in which continuous precipitation also occurs (Fig. 1a). Prior to the completion of the first reaction, secondary cells of much coarser spacing and much thicker thickness of  $\alpha$  and  $\gamma$  lamellae form at the original grain

boundaries and advance into the first cells (Fig. 1b, c). The region near the advancing interfaces of the primary cells can also be recognized as lamellar structure, with coarser spacing (Fig. 1c). However, these structures are not related to the secondary reaction but to divergent lamellar structure which forms accompanying the cell growth of the first reaction. These divergent phenomena were attributed to the effect of continuous precipitation on the cell growth of discontinuous precipitation, as discussed previously [21–23]. As the ageing temperature increases (Fig. 1d) and the Be content decreases (Fig. 1e), the secondary cells have a wider interlamellar spacing; however, the lamellar nature decreases. Furthermore, the lamellar structure cannot be observed in the secondary cells in Cu–9.8% Be alloy aged at 773 K (Fig. 1f).

#### 3.2. Micro-Vickers hardness measurement

A typical relationship between the hardness and ageing time is shown in Fig. 2. At shorter ageing times, the hardness increases from  $H_v = 100$  (as-quenched value)

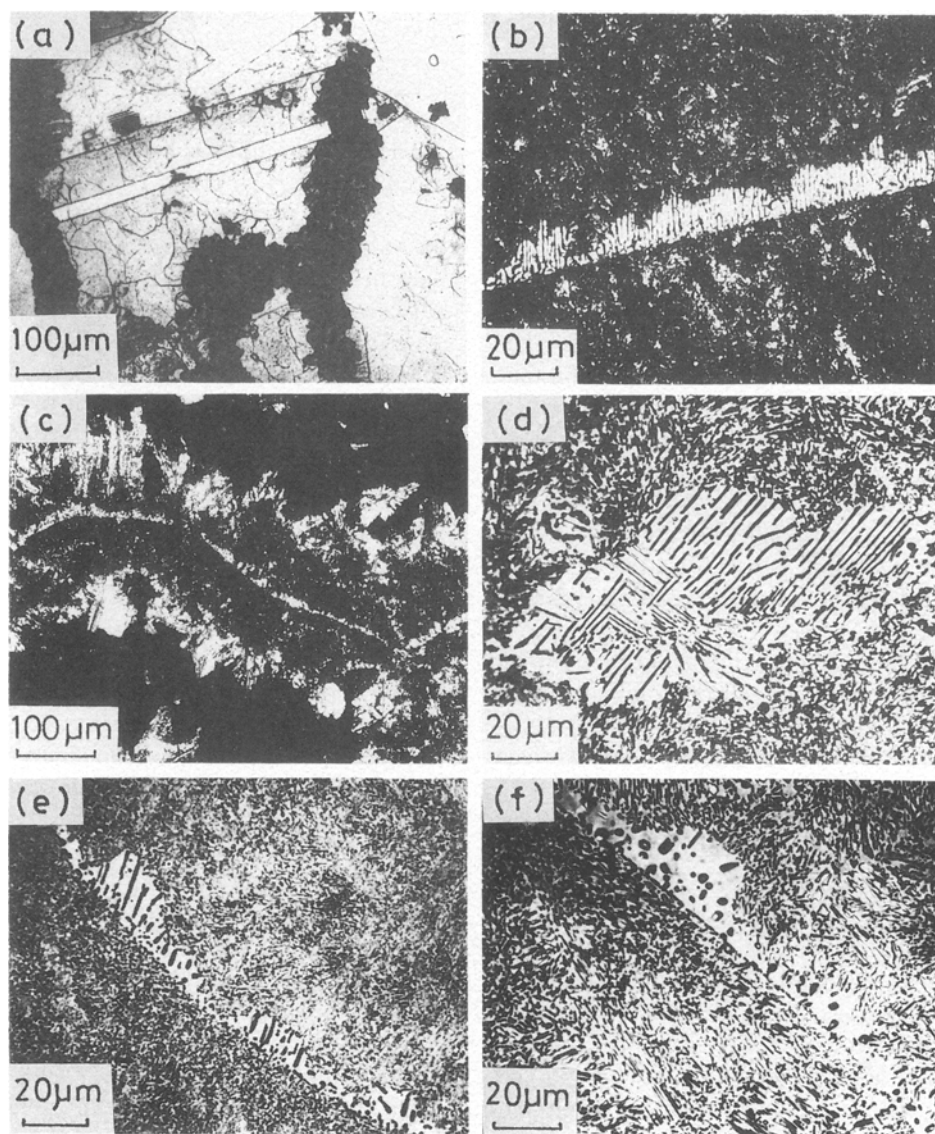


Figure 1 Typical microstructures of first and secondary reactions. (a)–(d) Cu–13.4% Be alloy; (e), (f) Cu–9.3% Be alloy. (a) aged for 180 s at 723 K, (b) aged for 140 ks at 723 K, (c) aged for 950 ks at 723 K, (d) aged for 1.82 Ms at 773 K, (e) aged for 840 ks at 723 K, (f) aged for 930 ks at 773 K.

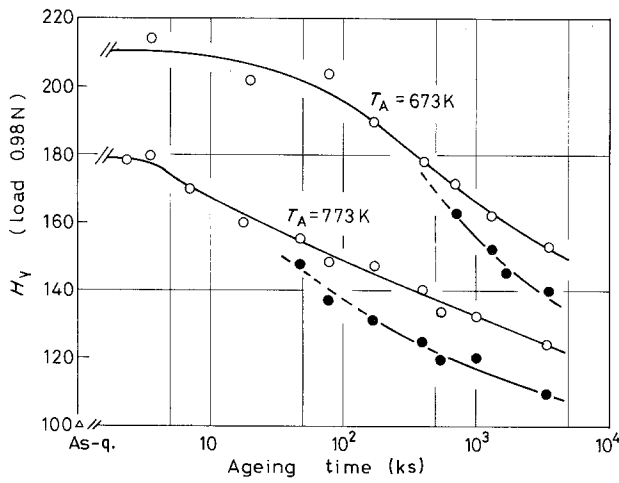


Figure 2 Relationship between ageing hardness of (○) first and (●) secondary reactions and ageing time (Cu-13.4% Be alloy).

to  $H_v = 210$  on ageing at 673 K and to  $H_v = 180$  on ageing at 773 K. This increase is attributed to the formation of the discontinuous precipitation (the first reaction) [21–23]. After attaining maximum hardness, the hardness of the primary cells decreases gradually with ageing time. During these softening processes, the secondary reaction occurs and the softening rate of the secondary cells is much faster than that of primary cells.

### 3.3. Cell radius and interlamellar spacing

The relationship between the radius of secondary cells and ageing time is shown in Fig. 3. The cell growth rate,  $G$ , is given by a slope of tangent to these curves.  $G$  decreases with ageing time at all ageing temperatures.

The relationship between the interlamellar spacing,  $l$  and ageing time in primary and secondary cells is shown in Fig. 4.  $l$  of the primary cells increases with ageing time. These results are important for the secondary reaction, because the secondary cells advance into the primary cells. The cell growth parameters of the first and secondary reactions and the coarsening ratio ( $l_2/l_1$ ) are summarized in Table I. Although the ratio tends to decrease with ageing temperature and increase with ageing time, the ratio is in the range 4–8.

### 3.4. Be contents in $\alpha$ phase

The measured volume fractions of  $\gamma$  phase within cells,  $f_\gamma$ , of the first and secondary reactions at various ageing stages are shown in Table II. The Be concentration of the  $\alpha$  phase,  $C_\alpha$ , was calculated from  $f_\gamma$  through the following equation

$$C_\alpha = C_0 \frac{V_\alpha}{V_\gamma} \frac{f_\gamma}{1 - f_\gamma} (C_0 - C_\gamma) \quad (1)$$

where  $C_0$  is the Be concentration in the alloy (0.134),  $C_\gamma$  the Be concentration in the  $\gamma$  phase (0.485 [24])\* ,  $V_\alpha$  the molar volume of  $\alpha$  phase ( $6.9 \times 10^{-6} \text{ m}^3 \text{ mol}^{-1}$ ), and  $V_\gamma$  the molar volume of  $\gamma$  phase ( $5.9 \times 10^{-6} \text{ m}^3 \text{ mol}^{-1}$ ). During the initial cell growth stage

\* The lattice parameter of the  $\gamma$  phase (0.2695 nm) is constant over this experimental ageing time.

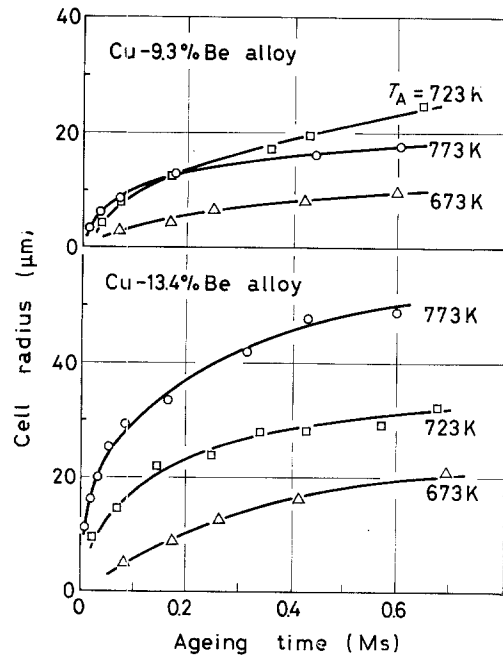


Figure 3 Relationship between cell radius of secondary reaction and ageing time.

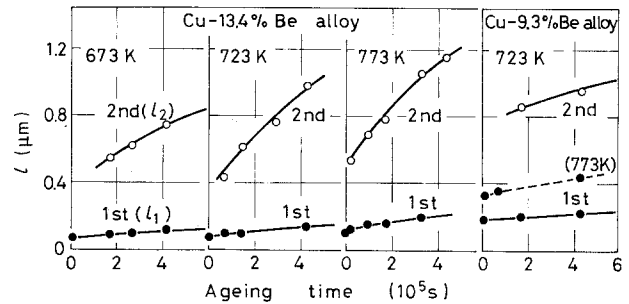


Figure 4 Relationship between interlamellar spacing of first ( $l_1$ ) and secondary ( $l_2$ ) reactions and ageing time.

of discontinuous precipitation (first reaction),  $C_\alpha$  is higher than  $C_\alpha^e$  (equilibrium Be content of  $\alpha$  phase [24]), i.e. supersaturated  $\alpha$  phase, as shown in an earlier study [21]. But  $C_\alpha$  in the first reaction decreases gradually with ageing time, eventually reaching  $C_\alpha^e$ .

The secondary cells advance after the ageing stage at which  $C_\alpha$  in the primary cells reaches  $C_\alpha^e$ , on ageing at 673 and 723 K. On ageing at 773 K,  $C_\alpha$  attains already  $C_\alpha^e$  even in the initial ageing stage of the first reaction. This will be due to the higher diffusivity of Be in the  $\alpha$  phase at 773 K.

### 3.5. Effect of cold work on secondary cell growth

Fig. 5 shows the typical microstructures of Cu-13.4% Be alloy cold rolled and reaged at 773 K. The secondary cells (white regions) of cold rolled specimens, also form at grain boundaries and advance into primary cells. In addition to these cells, however, other white regions appear within the primary cells and spread

TABLE I Cell growth parameters and coarsening ratio ( $l_2/l_1$ )

Alloy	$T_A$ (K)	$t$ (ks)	$l_1$ ( $10^{-7}$ m)	$l_2$ ( $10^{-7}$ m)	$l_2/l_1$	$G_2$ ( $10^{-11}$ m s $^{-1}$ )
9.8 % Be	723	2.2	1.56	—	—	—
		173	1.94	8.6	4.4	3.19
		432	2.22	9.55	4.3	2.11
		648	2.37	11.6	4.9	2.08
13.4 % Be	673	0.6	0.62	—	—	—
		173	0.94	5.0	5.3	4.58
		266	1.05	5.9	5.6	3.11
		418	1.08	6.2	6.7	2.25
		698	1.11	9.5	8.6	1.19
	723	0.2	0.765	—	—	—
		18.9	0.88	3.2	3.6	25
		68.4	1.07	4.19	3.9	11
		140	0.98	6.10	6.2	5.7
		428	1.34	9.85	7.4	1.5
		680	1.66	12.1	7.3	0.94
		773	0.12	0.895	—	—
	773	18	1.41	5.33	3.8	28.2
		82.8	1.57	6.93	4.4	9.44
		171	1.60	7.74	4.8	7.5
319		2.03	10.5	5.2	4.86	

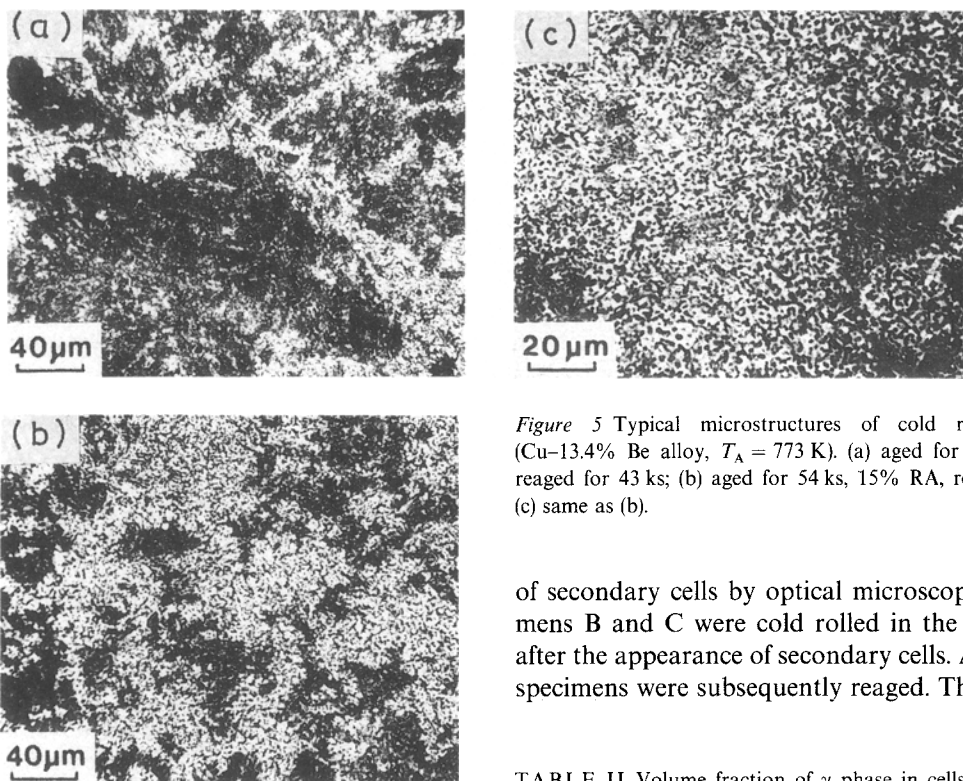


Figure 5 Typical microstructures of cold rolled specimens (Cu-13.4% Be alloy,  $T_A = 773$  K). (a) aged for 54 ks, 15% RA, reaged for 43 ks; (b) aged for 54 ks, 15% RA, reaged for 108 ks; (c) same as (b).

of secondary cells by optical microscopy, and Specimens B and C were cold rolled in the ageing stages after the appearance of secondary cells. All cold rolled specimens were subsequently reaged. The broken line

into the cells (Fig. 5b). Even by SEM, no distinct interface between the white and black regions was observed. These white regions contain spheroidized particles rather than lamellar precipitates (Fig. 5c). The white structures are considered to be produced not by the discontinuous coarsening reaction but by continuous coarsening reaction within the lamellar structure of first cells.

Fig. 6a shows the relation between the hardness and ageing time on cold rolled specimens. Specimen A was cold rolled in the ageing stage before the appearance

TABLE II Volume fraction of  $\gamma$  phase in cells,  $f_\gamma$ , Be concentration of  $\alpha$  phase in cells,  $C_\alpha$ , evaluated from Equation 1 and equilibrium Be concentration in  $\alpha$  phase,  $C_\alpha^e$  [24]. (Cu-13.4% Be alloy)

$T_A$ (K)	$t$ (ks)	Reaction	$f_\gamma$	$C_\alpha$	$C_\alpha^e$
673	0.54	1st	0.173	0.049	
	14.4	1st	0.192	0.038	
	64.8	1st	0.203	0.029	0.028
		2nd	0.205	0.027	
723	0.24	1st	0.159	0.056	
	24.5	1st	0.189	0.041	0.044
		2nd	0.188	0.040	
773	0.18	1st	0.149	0.062	0.06

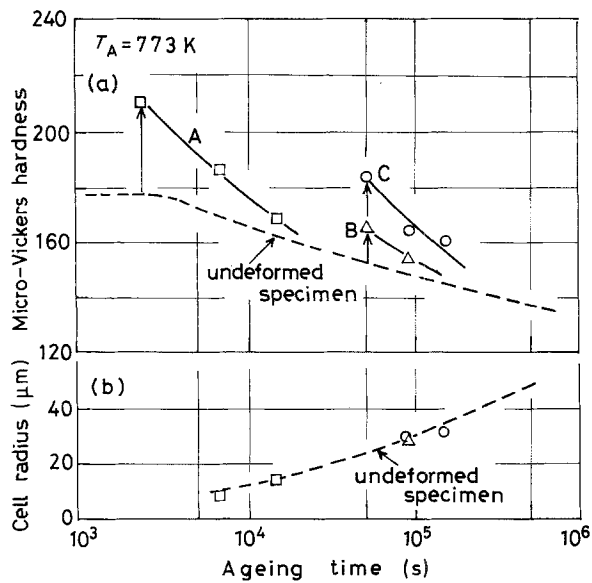


Figure 6 (a) Hardness and (b) cell radius of cold rolled specimens (Cu-13.4% Be alloy). A, aged 24 ks, RA 20%; B, aged 54 ks, RA 5%; C, aged 54 ks, RA 15%.

in this figure shows the relation between the hardness of the primary cells in the undeformed specimens; the cold rolled specimens are harder but soften quicker with ageing time.

Fig. 6b shows the relationship between the cell radius of the secondary reaction in cold rolled specimens and ageing time. The broken line again represents the same relation as shown in Fig. 3. All cell radii of cold rolled specimens fall on the broken line. Therefore, there is no effect of deformation on the cell growth rate of the secondary reaction.

#### 4. Discussion

From Table II, it is seen that  $C_\alpha$  in the primary cells decreases with ageing time and eventually reaches  $C_\alpha^c$ . This process of decreasing Be content within the  $\alpha$  lamella may be treated by the following equation [25]

$$\frac{C_1 - C_\alpha^c}{C_0 - C_\alpha^c} = \exp\left(-\pi^2 \frac{Dt}{l^2}\right) \quad (2)$$

where,  $C_1$  is the Be concentration in the  $\alpha$  phase within the primary cells at ageing time,  $t$ ,  $C_0$  is assumed to be the Be concentration in the  $\alpha$  phase at the initial cell growth stage of primary cells, and  $D$  is the volume diffusion coefficient of Be in the  $\alpha$  phase. The calculated  $D$ -value at 673 K was  $2-6 \times 10^{-19} \text{ m}^2 \text{ s}^{-1}$  which is in agreement with the values of  $D$  of Be in  $\alpha$  Cu-Be ( $6 \times 10^{-19} \text{ m}^2 \text{ s}^{-1}$  [26]) and  $D$  of Be in Cu ( $4 \times 10^{-20} \text{ m}^2 \text{ s}^{-1}$  [27]), obtained by extrapolation down to 673 K.

The secondary cells advance after the ageing stage at which  $C_\alpha$  of the primary cells reaches  $C_\alpha^c$ . Therefore, it can be concluded that there is no chemical free energy change accompanying the secondary cell growth in this alloy. This conclusion is different from those in other alloys [9-14]. In these references, the solute content of the depleted phase might be obtained from the specimens aged for a short time to give the primary cells, and for a long time to give the secondary

cells. Furthermore, there is no information on the variation of  $C_\alpha$  with ageing time in these references.

From a study of the effect of cold work on the cell growth of the secondary reaction, it is concluded that there is no effect of plastic deformation up to 20% RA on the cell growth rate in both ageing stages of the initial and the secondary reactions. This conclusion is in contrast to the results on discontinuous precipitation [28]. These differences may be explained by the different driving forces between discontinuous precipitation and the discontinuous coarsening reaction. Cold work introduces many lamellar faults in the primary cells and further, these faults will be introduced heterogeneously because the RA is relatively small. The lamellar faults play an important role in the continuous coarsening reaction [29], which results in the formation of spheroidized structure, as shown in Fig. 5c.

These continuous coarsening phenomena were also observed in undeformed specimens. For example, the interlamellar spacing of primary cells increases with ageing time. This increase is not related to the divergent phenomena of primary cells, because the data on lamellar spacing in this study were obtained from the regions close to the original grain boundaries and/or advancing interfaces of secondary cells, and the divergence occurred at much larger cell radius of the first reaction ( $R$  as shown in Fig. 7) than that of the secondary reaction [22, 23], i.e. the interlamellar spacing of cells less than  $R$  was independent of cell growth stage. Hence, the softening of primary cells shown in Fig. 2 is mainly due to the continuous coarsening reaction. The decrease in  $G$  and increase in  $l$  with ageing time for secondary cells are also attributed to this continuous coarsening reaction of the primary cells where the secondary cells advance. This continuous coarsening reaction has been studied in eutectic [19] and eutectoid [20] systems, but there is limited information on discontinuous precipitation systems.

From the above, it is concluded that the driving force for the secondary reaction is the reduction in total interlamellar surface energy accompanying the secondary reaction.

#### 5. Conclusions

1. When discontinuous precipitation is nearly complete, a discontinuous coarsening reaction with a much coarser interlamellar spacing begins at the original grain boundaries and advances into the primary cells.

2. The cell growth rate decreases and the interlamellar spacing increases with ageing time for the discontinuous coarsening reaction. These phenomena can be attributed to the continuous coarsening reaction which occurs in the primary cells prior to the advancement of secondary cells.

3. The  $\alpha$  phase in the primary cells supersaturates at the initial ageing stages of discontinuous precipitation (first reaction), but attains the equilibrium value prior to the appearance of the discontinuous coarsening cells.

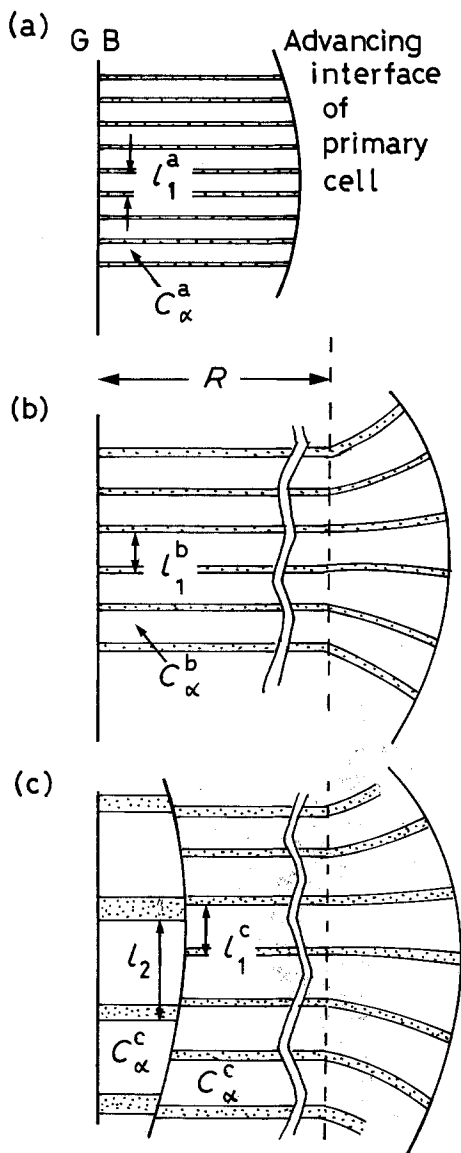


Figure 7 Schematic representation showing cell growth morphologies of first and secondary reactions.  $R$  is the largest cell radius of first reaction at which the cell growth and interlamellar spacing are independent of ageing time. (a) Initial cell growth stage of first reaction, (b) relatively later cell growth stage of first reaction, (c) cell growth stage of secondary reaction.  $l_1^a < l_1^b < l_1^c$ ,  $C_\alpha^a > C_\alpha^b > C_\alpha^c = C_\alpha^c$ . GB = grain boundary.

4. The decrease in Be content of the  $\alpha$  phase is controlled by volume diffusion of Be in partially depleted  $\alpha$  phase.

5. The driving force for the discontinuous coarsen-

ing reaction is the reduction in the total interlamellar surface energy.

## References

1. M. FREBEL and B. OTTE, *Scripta Metall.* **9** (1975) 1317.
2. J. J. JANECEK and B. J. PLETKA, in "Solid  $\rightarrow$  Solid Phase Transformations", edited by H. I. Aaronson, D. E. Laughlin, R. F. Sekerka and C. M. Wayman (TMS-AIME, Warrendale, 1982) p. 963.
3. M. KAYA and R. W. SMITH, *Acta Metall.* **37** (1989) 1657.
4. *Idem.*, *ibid.* **37** (1989) 1667.
5. D. CHEETHAM and N. RIDLEY, *J. Inst. Metals* **99** (1971) 371.
6. J. D. LIVINGSTON and J. W. CAHN, *Acta Metall.* **22** (1974) 495.
7. C. W. SPENCER and D. J. MACK, in "Solid  $\rightarrow$  Solid Phase Transformations", edited by H. I. Aaronson, D. E. Laughlin, R. F. Sekerka and C. M. Wayman (TMS-AIME, Warrendale, 1982) p. 549.
8. H. TSUBAKINO, R. NOZATO and K. ISHIGURO, *J. Jpn Inst. Metals* **44** (1980) 1127.
9. S. P. GUPTA, *Acta Metall.* **35** (1987) 747.
10. B. PREDEL and M. FREBEL, *ibid.* **20** (1972) 259.
11. R. A. FOURNELLE, *ibid.* **27** (1979) 1135.
12. *Idem.*, *ibid.* **27** (1979) 1147.
13. G. SPEICH, *Trans. Metall. Soc. AIME* **20** (1972) 259.
14. C. P. JU and R. A. FOURNELLE, *Acta Metall.* **33** (1985) 71.
15. J. PETERMANN and E. HORNBOGEN, *Z. Metallkde* **59** (1968) 814.
16. H. TSUBAKINO and R. NOZATO, in "Solid  $\rightarrow$  Solid Phase Transformations", edited by H. I. Aaronson, D. E. Laughlin, R. F. Sekerka and C. M. Wayman (TMS-AIME, Warrendale, 1982) p. 951.
17. H. TSUBAKINO, *J. Mater. Sci. Lett.* **1** (1982) 306.
18. H. BORCHERS and H. SCHULZ, *Z. Metallkde* **66** (1975) 525.
19. L. D. GRAHAM and R. W. KRAFT, *ibid.* **57** (1966) 94.
20. B. G. MELLOR, P. V. EDMONDS and G. A. CHADWICK, *Metal Sci.* **12** (1978) 439.
21. H. TSUBAKINO and R. NOZATO, *J. Jpn Inst. Metals* **43** (1979) 42.
22. *Idem.*, *Bull. Univ. Osaka Pref.* **A21** (1981) 153.
23. H. TSUBAKINO, R. NOZATO and H. HAGIWARA, *Trans. Jpn Inst. Metals* **22** (1981) 153.
24. M. HANSEN and K. ANDERKO, "Constitution of Binary Alloys" (McGraw-Hill, New York, 1958) p. 281.
25. D. TURNBULL, in "Defects in Crystalline Solids", Report of the Bristol Conference (Physics Society, London, 1954) p. 203.
26. R. REINBACH and F. KRIETSH, *Z. Metallkde* **54** (1963) 173.
27. R. L. FOGEL'SON, YA. A. UGAY, A. V. POKOYEV, I. A. AKIMOV and V. D. KRETININ, *Phys. Metals Metallogr.* **35** (1973) 176.
28. H. KREYE, *Z. Metallkde* **62** (1971) 556.
29. K. A. JACKSON and J. D. HUNT, *Trans. Metall. Soc. AIME* **62** (1971) 556.

Received 29 August 1989

and accepted 2 October 1990